A 2.5D coupled FE-BE methodology for the prediction of railway induced vibrations

Stijn François[1], Pedro Galvín[1,2], Mattias Schevenels[1], Geert Lombaert[1] and Geert Degrande[1]

Abstract Ground vibrations induced by railway traffic are often studied by means of two-and-half dimensional (2.5D) models that are based on the longitudinal invariance of the track geometry. In this paper, a 2.5D methodology is used where the finite element method is combined with a boundary element method, based on a regularized boundary integral equation. In the formulation of the boundary integral equation, the Green's functions of a layered elastic halfspace are used, so that no discretization of the free surface or the layer interfaces is required. The methodology is applied to two cases. In the first case, two alternative models for a ballasted track on an embankment are compared. In the first model, the ballast and the embankment are modelled as a continuum using 2.5D solid elements, whereas a simplified beam representation is adopted in the second model. A very large difference is found for the free field mobility of both models, which demonstrates the need for detailed 2.5D modelling of the embankement. In the second case, the efficiency of a vibration isolating screen is studied. A vibration isolating screen is a soft or stiff wave barrier. Due to the impedance contrast between the isolating screen and the soil, incident waves are reflected. As a result, the vibration levels behind the screen are effectively reduced. Both examples demonstrate that the use of detailed 2.5D models result in a better insight in the mechanical behavior of the coupled soil-track system.

1 Introduction

For the prediction of railway induced vibrations, the geometry of the track-soil system is often assumed to be invariant in the longitudinal direction [7]. This allows

[1]Department of Civil Engineering, K.U.Leuven, Kasteelpark Arenberg 40, B-3001 Leuven, Belgium. e-mail: stijn.francois@bwk.kuleuven.be
[2] Escuela Técnica Superior de Ingenieros, Universidad de Sevilla, Camino de los Descubrimientos, E-41092 Sevilla, Spain.

for a Fourier transform of the coordinate in the longitudinal direction of the track and leads to a solution in the frequency-wavenumber domain where the original three-dimensional (3D) problem is replaced by a two-dimensional (2D) problem for each wavenumber. This two-and-half dimensional (2.5D) methodology results in a considerable reduction of the computation time [2, 7] compared to full 3D models.

Recently, a novel 2.5D FE-BE methodology has been proposed by François et al. [2]. The 2.5D FE-BE methodology combines the classical 2.5D FE method with a novel 2.5D BE method, based on a regularized boundary integral equation in terms of the Green's functions of a layered halfspace.

In this paper, the 2.5D coupled FE-BE models is applied to the prediction of railway traffic induced vibrations. Two cases are considered. In the first case, two alternative models for a ballasted track on an embankment are compared. The 2.5D BE-FE method is used to model the ballast and the embankment as an elastic continuum, as an alternative to simplified ballast and embankment models used in the literature [5, 7]. In the second case, the efficiency of a vibration isolating screen is studied.

2 Methodology

The dynamic interaction between a railway track and the underlying soil is a problem of dynamic soil–structure interaction. A domain decomposition method is used to solve the problem, where the subdomain Ω_b represents the structure and the subdomain Ω_s the soil (figure 1). It is assumed that the geometry of the track is invariant

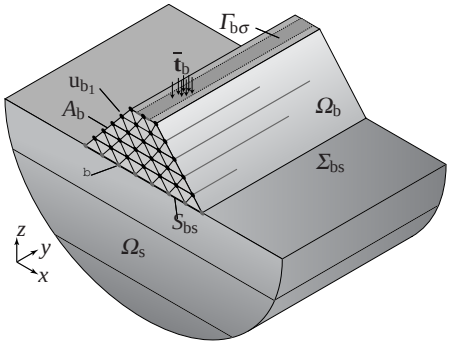

Fig. 1 The geometry of the coupled soil-structure system.

with respect to the coordinate y in the longitudinal direction. The soil is modelled as a horizontally layered halfspace and, therefore, invariant with respect to the y-direction as well. The dynamic track-soil interaction problem is assumed to be linear and all equations are elaborated using virtual work in the frequency domain.

The equilibrium equation for the dynamic soil-structure interaction problem is formulated in a variational form. For any virtual displacement field $\mathbf{v}_\mathrm{b}$ imposed on the structure Ω_b, the sum of the virtual work of the internal and the inertial forces is equal to the virtual work of the external loads:

$$-\omega^2 \int_{\Omega_\mathrm{b}} \mathbf{v}_\mathrm{b} \cdot \rho_\mathrm{b} \mathbf{u}_\mathrm{b} d\Omega + \int_{\Omega_\mathrm{b}} \boldsymbol{\varepsilon}_\mathrm{b}(\mathbf{v}_\mathrm{b}) : \boldsymbol{\sigma}_\mathrm{b}(\mathbf{u}_\mathrm{b}) d\Omega = \int_{\Omega_\mathrm{b}} \mathbf{v}_\mathrm{b} \cdot \rho_\mathrm{b} \mathbf{b}_\mathrm{b} d\Omega + \int_{\Gamma_{\mathrm{b}\sigma}} \mathbf{v}_\mathrm{b} \cdot \bar{\mathbf{t}}_\mathrm{b}^{\mathbf{n}_\mathrm{b}} d\Gamma + \int_{\Sigma_\mathrm{bs}} \mathbf{v}_\mathrm{b} \cdot \mathbf{t}_\mathrm{b}^{\mathbf{n}_\mathrm{b}}(\mathbf{u}_\mathrm{b}) d\Gamma \quad (1)$$

where $\mathbf{u}_\mathrm{b}$ is the displacement vector in the structure, $\rho_\mathrm{b}\mathbf{b}_\mathrm{b}$ denotes the body force in the domain Ω_b, and $\mathbf{t}_\mathrm{b}^{\mathbf{n}_\mathrm{b}} = \sigma_\mathrm{b} \cdot \mathbf{n}_\mathrm{b}$ is the traction vector on a boundary with unit outward normal vector $\mathbf{n}_\mathrm{b}$ (figure 1). Tractions $\bar{\mathbf{t}}_\mathrm{b}^{\mathbf{n}_\mathrm{b}}$ are imposed on the boundary $\Gamma_{\mathrm{b}\sigma}$.

Accounting for the equilibrium of stresses on the interface Σ_bs and using a 2.5D finite element formulation for the interpolation of the displacement field with respect to the coordinates x and z, equation (1) can be elaborated as [2]:

$$\left[-\omega^2 \mathbf{M}_\mathrm{bb} + \mathbf{K}_\mathrm{bb}^0 - ik_y \mathbf{K}_\mathrm{bb}^1 - k_y^2 \mathbf{K}_\mathrm{bb}^2 + ik_y^3 \mathbf{K}_\mathrm{bb}^3 + k_y^4 \mathbf{K}_\mathrm{bb}^4 + \mathbf{K}_\mathrm{bb}^\mathrm{s}(k_y,\omega)\right] \tilde{\mathbf{u}}_\mathrm{b}(k_y,\omega) = \tilde{\mathbf{f}}_\mathrm{b}(k_y,\omega) \quad (2)$$

where $\mathbf{K}_\mathrm{bb}^0$, $\mathbf{K}_\mathrm{bb}^1$, $\mathbf{K}_\mathrm{bb}^2$, $\mathbf{K}_\mathrm{bb}^3$ and $\mathbf{K}_\mathrm{bb}^4$ are the stiffness matrices, $\mathbf{M}_\mathrm{bb}$ is the mass matrix, $\tilde{\mathrm{f}}_\mathrm{b}(k_y,\omega)$ is the external load vector, and $\mathbf{K}_\mathrm{bb}^\mathrm{s}(k_y,\omega)$ represents the dynamic soil stiffness matrix. A tilde above a variable denotes its representation in the frequency-wavenumber domain. The finite element matrices $\mathbf{M}_\mathrm{bb}$ and $\mathbf{K}_\mathrm{bb}^0$ to $\mathbf{K}_\mathrm{bb}^4$ in equation (2) are independent of the wavenumber k_y and the frequency ω and are only assembled once.

The dynamic soil stiffness matrix $\mathbf{K}_\mathrm{bb}^\mathrm{s}(k_y,\omega)$ is computed by means of a 2.5D boundary element method, where a regularized version [2] of the 2.5D boundary integral equation is applied. In the formulation of the boundary integral equation, the Green's functions of a layered elastic halfspace [6] are used, so that no discretization of the free surface or the layer interfaces is required. Both the 2.5D finite element and boundary element methods have been implemented in MATLAB using a C++ mex interface.

3 A ballasted track on an embankment

In this section, the proposed 2.5D FE-BE model is used to predict the transfer functions between the track and free field at a site in Reugny (France) situated along the high speed railway line LGV Atlantique. The track in Reugny is a classical ballasted track, situated on top of an embankment. The continuously welded UIC60 rails are supported by rail pads and fixed with clips on twin block concrete sleepers with a spacing of $d = 0.60\,\mathrm{m}$. The concrete twin block sleepers have a length $l_\mathrm{sl} = 2.41\,\mathrm{m}$ and are composed of two tied concrete blocks with a length $l_\mathrm{bl} = 0.84\,\mathrm{m}$. The total

mass of the sleepers $m_{sl} = 250\,\text{kg}$. The track is supported by a ballast layer with a thickness $h_b = 0.30\,\text{m}$ and a density $\rho_b = 1400\,\text{kg/m}^3$. The embankment has a width $w_{e1} = 6\,\text{m}$ at the top supporting the railway track, a width $w_{e2} = 13\,\text{m}$ at the soil's surface, and a height $h_e = 2\,\text{m}$.

Two alternative track models are considered. In the first model (figure 2a), the ballast and the embankment are modelled as an elastic continuum using 2.5D solid elements. The second model (figure 2b) is a simplified model where the ballast is represented by distributed springs and dampers while the embankment is modelled as an Euler-Bernoulli beam. Similar simplified models of the ballast and the embankment are frequently used for the prediction of railway induced vibrations [5, 7].

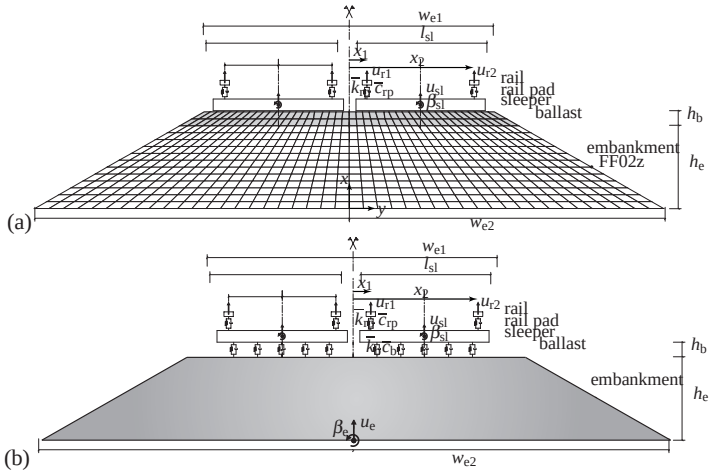

Fig. 2 Cross section of (a) model 1 and (b) model 2 of the ballasted track on the embankment.

In both models, the rails are represented by Euler-Bernoulli beams. The positions of the rail are determined by $x_1 = 1.145\,\text{m}$ and $x_2 = 2.580\,\text{m}$, with $x_2 - x_1$ equal to the track gauge r_d. The internal energy dissipation in the rail is modelled by a loss factor $\eta_r = 0.05$. The rail pads are modelled as continuous spring-damper connections. The rail pad stiffness k_{rp} of a single rail pad is used to calculate an equivalent stiffness $\overline{k}_{rp} = k_{rp}/d = 130 \times 10^6\,\text{N/m}^2$. A loss factor $\eta_{rp} = 0.23$ is used to account for internal energy dissipation in the rail pad.

The concrete sleepers are assumed to be rigid in the plane of the track cross section and are modelled as a uniformly distributed mass $\overline{m}_{sl} = m_{sl}/d$ of $417\,\text{kg/m}$. The sleeper's rotational inertia $\rho_{sl}\overline{I}_{sl} = \rho_{sl}I_{sl}/d$ has been estimated as $298\,\text{kgm}^2/\text{m}$ taking into account the excentric position of the two blocks.

In model 1, the ballast bed is modelled as an elastic continuum, using 88 2.5D solid elements [2]. The ballast has a Young's modulus $E_b = 111 \times 10^6\,\text{N/m}^2$, a Poisson's ratio $\nu_b = 0.36$, a density $\rho_b = 1550\,\text{kg/m}^3$, and a loss factor $\eta_b = 1.00$.

The embankment is modelled as an elastic continuum using 528 2.5D solid elements and has A Young's modulus $E_e = 170 \times 10^6\,\mathrm{N/m^2}$, Poisson's ratio $\nu_e = 0.36$, and a density $\rho_e = 1400\,\mathrm{kg/m^3}$.

In model 2, the ballast is represented by a set of distributed linear springs and dampers. The smeared ballast stiffness $\overline{k}_b$ is computed from the vertical spring stiffness k_b per sleeper [N/m] as k_b/d and equal to $300 \times 10^6\,\mathrm{N/m^2}$. The loss factor $\eta_b = 1.00$. The equivalent ballast mass $\overline{m}_b$ is computed from the ballast mass m_b situated under each sleeper as m_b/d. The ballast mass m_b is estimated from the height h_b of the ballast layer and a width $w_{b1} = l_{sl}$ and $w_{b2} = 3\,\mathrm{m}$ at the top and the bottom of the ballast layer, respectively, as $m_b = 0.5\rho_b h_b(w_{b1} + w_{b2})b_{bl}$. This leads to a value of $608\,\mathrm{kg/m}$ for the equivalent ballast mass $\overline{m}_b$. The embankment is represented by an Euler-Bernoulli beam, which implies that the cross section of the embankment is assumed to be rigid.

The soil is modelled as a horizontally layered elastic halfspace, with a single layer with a thickness of $2.0\,\mathrm{m}$ and a shear wave velocity $C_s = 211\,\mathrm{m/s}$ on top of a halfspace with a shear wave velocity of $403\,\mathrm{m/s}$. These properties have been obtained from a Spectral Analysis of Surface Waves test on site. The density ρ is equal to $1400\,\mathrm{kg/m^3}$ for the top layer and equal to $2650\,\mathrm{kg/m^3}$ for the underlying halfspace. The Poisson's ratio ν is 0.36 for the top layer and 0.16 for the halfspace. The material damping ratio β in both deviatoric and volumetric deformation has a value of 0.05 and 0.06 for the top layer and the halfspace, respectively.

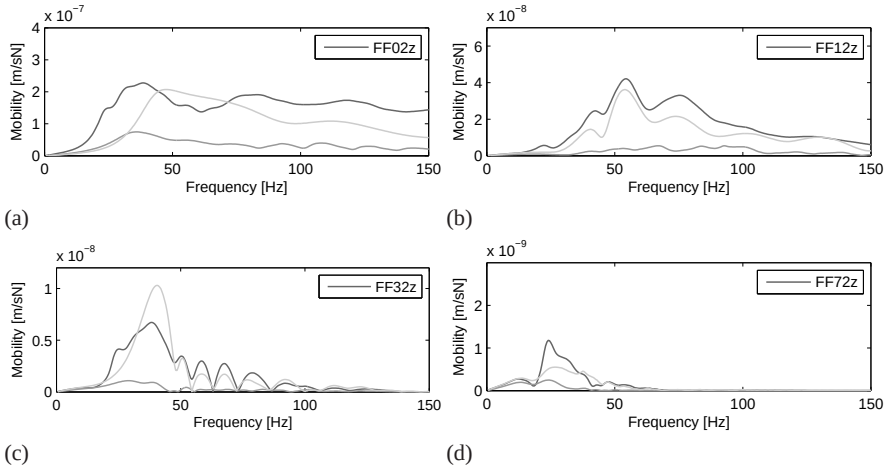

Fig. 3 Free field mobility at (a) 2 m, (b) 12 m, (c) 32 m, and (d) 72 m from the outer rail computed from model 1 (dark grey line), model 2 (grey line), and model 2 without embankment (light grey line).

Figure 3 compares the free field mobility at a distance of 2 m, 12 m, 32 m, and 72 m from rail 2 as computed with both models. The point located at 2 m from the outer rail is situated on the embankment.

A very large difference is found between both results. The assumption of an Euler Bernoulli model for the embankment leads to high tractions near the edges of the embankment, whereas in the case of the solid embankment model, the tractions are distributed more smoothly along the interface. As expected, model 1 leads to more accurate results as it allows for a better approximation of the stress distribution at the interface between the embankment and the soil.

At frequencies below 20 Hz, the free field mobility is similar for both models, whereas at higher frequencies the free field mobility obtained by model 1 is larger. This might be due to the fact that at low frequencies, the wavelength in the soil is large with respect to the width of the interface between the embankment and the soil, so that the differences in the traction distribution do not significantly affect the radiated wave field. At higher frequencies, the wavelengths are smaller, so that the free field mobility is sensitive to the differences in the traction distribution. The smaller value of the free field mobility for model 2 is probably due to the assumption of a rigid cross section for the embankment, which leads to very high values of the tractions near the edges of the embankment and, therefore, a substantial filtering effect when the wavelength in the soil is of the same order of magnitude as the width of the interface.

4 Vibration isolating screen

In this section, the 2.5D coupled FE-BE methodology is applied to study the efficiency of a vibration isolating screen in the soil. A vibration isolating screen is a soft or stiff wave barrier. Due to the impedance contrast between the isolating screen and the soil, waves are reflected, effectively reducing vibration levels behind the screen.

First, the reference case of a unit point load on the surface of a homogeneous halfspace is considered. The soil has a shear wave velocity $C_s = 150\,\mathrm{m/s}$, a dilatational wave velocity $C_p = 300\,\mathrm{m/s}$, a density $\rho = 1800\,\mathrm{kg/m^3}$ and a material damping ratio $\beta_s = \beta_p = 0.05$ in both deviatoric and volumetric deformation. The displacement in the soil is dominated by Rayleigh waves with cylindrical wave fronts and a velocity $C_R = 139.8\,\mathrm{m/s}$ which corresponds to a wavelength $\lambda_R = C_R/f = 6.95\,\mathrm{m}$ at the frequency $f = 20\,\mathrm{Hz}$ (figure 4a) and $\lambda_R = 3.48\,\mathrm{m}$ at a frequency $f = 40\,\mathrm{Hz}$ (figure 4b). The penetration depth of the Rayleigh waves is proportional to the wavelength: most of the wave energy is located above a depth of one wavelength. The embedment depth of the vibration isolating screen should therefore be larger than the penetration depth of the Rayleigh waves.

In the present case, a concrete vibration isolating screen with a depth of 8 m and a width of 0.6 m is considered, which is expected to isolate vibrations above a frequency of 20 Hz. The concrete has a Young's modulus $E_c = 30\,\mathrm{GPa}$, a Poisson's ratio $\nu_c = 0.2$ and a density $\rho_c = 2600\,\mathrm{kg/m^3}$. A vertical point source is considered

at the surface of the halfspace at a distance of 5 m from the centerline of the screen. Figures 4c and 4d show the real part of the vertical displacement in the free field at frequencies of 20 Hz and 40 Hz, respectively. The incident waves are reflected on the vibration isolating screen, reducing vibration levels behind the screen. At 40 Hz, two lines of destructive interference between a direct and reflected Rayleigh waves are observed. As the concrete is much stiffer than the soil, it acts as a rigid wave barrier and a small displacement amplitude is observed along the soil-screen interface. The

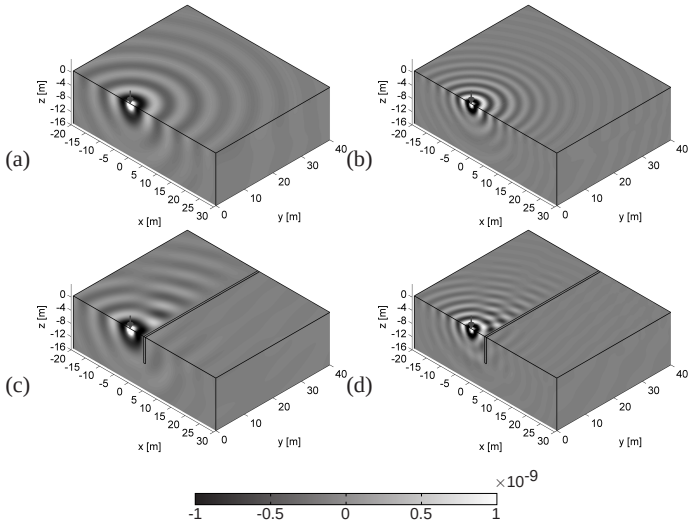

Fig. 4 Real part of the vertical displacement for a unit harmonic point load for a unit vertical point load at the surface of a homogeneous halfspace at a frequency of (a) 20 Hz and (b) 40 Hz and at distance of 5 m from the center of the concrete vibration isolating screen at a frequency of (c) 20 Hz and (d) 40 Hz.

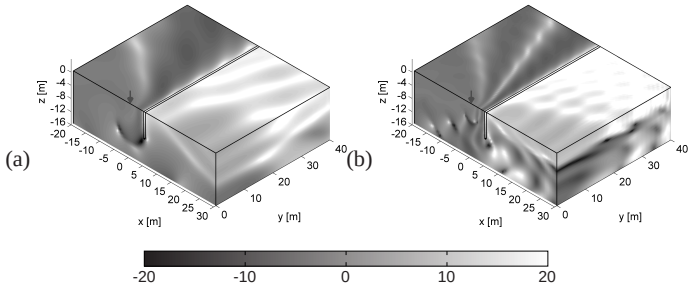

Fig. 5 Vertical insertion loss IL_z for a harmonic point load at a distance $d = 5$ m from the vibration isolating screen at a frequency of (a) 20 Hz and (b) 40 Hz for a concrete vibration isolating screen.

efficiency of the vibration isolating screen can also be quantified by the insertion

loss $\mathrm{IL}_z = 20\log_{10}(\frac{|u_z^{\mathrm{uniso}}(\omega)|}{|u_z^{\mathrm{iso}}(\omega)|})$ of the vertical displacement, defined as the ratio of the vertical displacement amplitudes $|u_z^{\mathrm{iso}}(\omega)|$ and $|u_z^{\mathrm{uniso}}(\omega)|$ in the case with and without vibration isolating screen. Figure 5 shows the vertical insertion loss at 20 Hz and 40 Hz. This indicates that the vibration isolating screen effectively reduces the vibration levels behind the trench. At 40 Hz, two lines of destructive interference between a direct and reflected Rayleigh waves are observed.

5 Conclusion

In this paper, the prediction of vibrations from a track on an embankment and a vibration isolating screen in the soil have been computed using a 2.5D coupled FE-BE methodology.

Two alternative models for a ballasted track on an embankment have been considered. In the first model, 2.5D solid elements are used to model the ballast and the embankment as a continuum, whereas in the second model a simplified representation is used. A considerable difference is observed in the free field mobility due to a different tractions distribution at the embankment-soil interface.

In the second case, a vibration isolating screen has been studied. Due to the impedance contrast between the isolating screen and the soil, incident waves are reflected and the vibration levels behind the screen are effectively reduced.

These examples demonstrate that the use of detailed 2.5D models result in a better insight in the mechanical behavior of the coupled soil-track system.

References

1. D. Aubry, D. Clouteau, and G. Bonnet. Modelling of wave propagation due to fixed or mobile dynamic sources. In N. Chouw and G. Schmid, editors, *Workshop Wave '94, Wave propagation and Reduction of Vibrations*, pages 109–121, Ruhr Universität Bochum, Germany, December 1994.
2. S. François, M. Schevenels, G. Lombaert, P. Galvín, and G. Degrande. A 2.5D coupled FE-BE methodology for the dynamic interaction between longitudinally invariant structures and a layered halfspace. *Computer Methods in Applied Mechanics and Engineering*, 199(23-24):1536–1548, 2010.
3. E. Kausel. *Fundamental solutions in elastodynamics: a compendium*. Cambridge University Press, New York, 2006.
4. E. Kausel and J.M. Roësset. Stiffness matrices for layered soils. *Bulletin of the Seismological Society of America*, 71(6):1743–1761, 1981.
5. G. Lombaert, G. Degrande, J. Kogut, and S. François. The experimental validation of a numerical model for the prediction of railway induced vibrations. *Journal of Sound and Vibration*, 297(3-5):512–535, 2006.
6. M. Schevenels, S. François, and G. Degrande. EDT: An ElastoDynamics Toolbox for MATLAB. *Computers & Geosciences*, 35(8):1752–1754, 2009.
7. X. Sheng, C.J.C. Jones, and M. Petyt. Ground vibration generated by a harmonic load acting on a railway track. *Journal of Sound and Vibration*, 225(1):3–28, 1999.